Hurst exponents and cyclic scenarios in a photonic integrated circuit

Konstantinos E. Chlouverakis, Apostolos Argyris, Adonis Bogris, and Dimitris Syvridis
Optical Communications Laboratory, Department of Informatics and Telecommunications, University of Athens, Panepistimiopolis, Illisia, Athens, 15784, Greece

(Received 30 June 2008; revised manuscript received 3 September 2008; published 23 December 2008)

We experimentally report the cyclic scenario of birth and annihilation of periodic orbits in a photonic integrated circuit as the feedback phase of the electric field varies. The latter is also shown to result in minimal alterations in the statistical properties of the chaotic attractor, with simultaneously transiting the Hurst exponent H, erratically, below and above the critical value of $H=0.5$ that indicates regular Brownian motion. Consequently there is an indication of the most effective operating regions with minimized predictability, which hinders eavesdropping and the progress of forecasting the development of the chaotic light carrier.

DOI: 10.1103/PhysRevE.78.066215 PACS number(s): 42.65.Sf, 42.82.Bq, 05.45.Tp, 82.40.Bj

The rekindled interest on the chaotic dynamics of semiconductor lasers is primarily ascribed to their innate aptitude of encrypting data on the physical layer [1,2]. In optical communications, chaotic carriers are most frequently generated using semiconductor lasers with optical injection [3], all-optical [4], and optoelectronic feedback [5]. The contemporary need for faster and additionally compact optical systems leads to the development of integrated photonics [6,7] that will be expectantly elevated to the verge of physical layer data encryption. The photonic integrated circuit (PIC) examined in this paper is identical with the one that was recently presented in Ref. [7] except for the distributed feedback (DFB) laser itself that acquired a higher linewidth enhancement factor, close to 8, due to 1572 nm wavelength operation instead of 1561 nm. In Ref. [7] the PIC's chaotic properties were examined regarding the calculation of chaoticity and complexity of the strange attractors, showing—under specific conditions—high-dimensional broadband chaos.

In this paper, we examine experimentally the effects of the feedback phase on the period-doubling cascades, on the statistical properties of chaotic carriers and on the latter's predictability. The concurrent birth and annihilation of periodic orbits is presented as the phase of the electric field varies. It is shown that the dynamics exhibit forward and inverse period doublings, together with windows of periodicity. Furthermore, the Hurst exponent H [8,9] of the electric field is calculated for the same range of the feedback phase indicating regions of $0.2<H<0.8$ for the chaotic cases. Analogous attempt for the calculation of the Hurst exponent took place in Ref. [10] but from different dynamics outlook, since H was calculated for the phase dynamics of the electric field that was derived mathematically with the Hilbert transform from experimentally recorded intensity series. Herein, we calculate H directly from the intensity (electric field) series and point out an indirect link with entropy.

The PIC examined herein consists of four successive sections depicted in Fig. 1: a DFB InGaAsP semiconductor laser operating at 1572 nm, followed by a gain-absorption section (G/As), a phase section (PHs), and a 1-cm-long passive waveguide (PW). The overall resonator length is defined by the internal laser facet and the chip facet of the waveguide which is highly reflective coated (HRC) ($R\approx 97\%$). Criterion of the selection of the cavity length is the ability of the device to produce chaotic dynamics [4,7]. The necessity of integrating a G/As outcomes from the requirement to control the optical feedback strength. For further details of the PIC see Ref. [7].

The phenomenon of forward and reverse period doublings is a scarcely frequent phenomenon for differential equations. It has been demonstrated theoretically and experimentally in electronic configurations [11], two-section lasers [12], and erbium doped fiber lasers. For all these examples see the references in Refs. [10,11]. For time-delayed systems, the cyclic scenario was experimentally demonstrated in Ref. [5] using optoelectronic feedback; however, this is the first experimental presentation, to our knowledge, of this phenomenon for an integrated semiconductor laser subjected to all-optical feedback. For an all-optical feedback experiment [13] this phenomenon was demonstrated, whereas though the cavity length was almost half of the one used herein and also comparable to its laser cavity length in contrast to the setup herein, therefore operating at nearly 800 μm wavelength and hence inappropriate for high-speed and long-haul telecommunications applications.

The laser is pumped at a current of $I=50$ mA ($3I_{TH}$) and the current of the G/As section is kept constant to $I_{G/As}=0$ mA. Hence the free control parameter throughout the experiment is the feedback phase controlled by the current I_{PHs} of the PHs. In Fig. 2 we present the time series of the electric amplitude from (a) to (h) for $I_{PHs}=4.1$ mA to 11.3 mA, where the system was found to enter and exit chaos via successive period-doubling cascades. For $4.1\ \text{mA}<I_{PHs}<5.2$ mA we noticed only limit cycles with periodicities up to 4. This is due to the stochastic noise sources that obviate the identification of periodic states with periodicities greater than 4 but also limit cycles with period 1 since noise adds slight peaks between two rotative extrema in a time series and hence visualization is addled. Nevertheless this transit to chaos is evidently a period-doubling one confirmed also from the power specta (not shown herein). While increasing I_{PHs} from 5.2 to 7.8 mA the PIC behavior was maintained fully chaotic and a window of periodicity appeared for $7.8\ \text{mA}<I_{PHs}<8.6$ mA which also experienced nearly intermittent behavior [Fig. 2(d)]; common feature for chaotic systems that exhibit this cyclic behavior [14]. With continuously increasing I_{PHs} chaotic persistent behavior was observed for $8.6\ \text{mA}<I_{PHs}<10$ mA and the system exits the chaotic re-

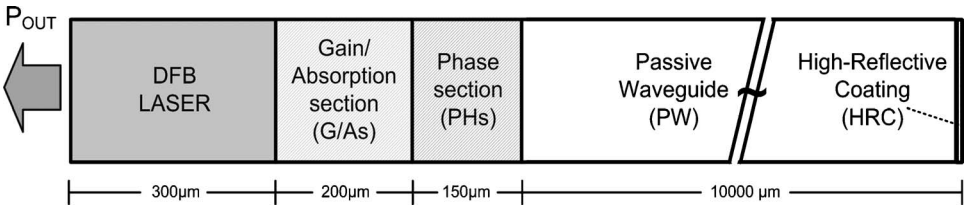

FIG. 1. Schematic diagram of the photonic integrated circuit.

gime with an inverse period-doubling route to chaos to CW operation finally at $I_{PHs}=11.3$ mA. It should be noted that the phenomenon of forward and reverse period doublings was present for laser currents $I<4I_{TH}$ and $I_{G/As}<0.5$ mA but absent for values greater than these (and especially the $I_{G/As}$) since persistent chaos behavior, independent of the feedback phase was observed. In Fig. 3 the zoomed cases for the beginning and ending of the period doubling cascades [of Figs. 2(b) and 2(g)] for the cyclic scenario are presented.

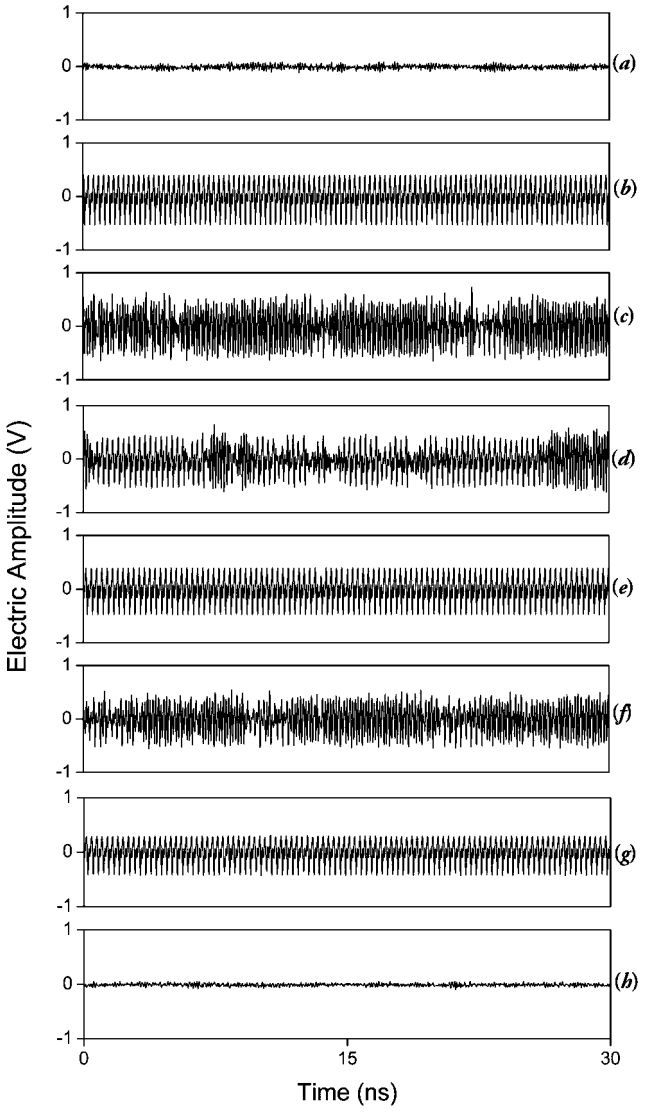

FIG. 2. Cyclic scenario: Experimental electric amplitude time-series with increasing the phase current I_{PHs} from (a) 4.1 mA to (h) 11.3 mA. The system starts from CW operation (a), enters chaos via period doubling cascades up to (c) showing also intermittent behavior (d), shows periodicity pockets in (e) and exits chaos via reverse period doublings until it reestablishes CW operation in (h).

Since the investigated PIC is fabricated for chaotic communications applications, it is prudent to examine the complexity of the resulted chaotic light carriers. In order for a carrier to be apt for encryption purposes, its chaotic properties should exhibit dynamics with high complexity (attractor dimension) and chaoticity (Kolmogorov entropy), as measured in Ref. [7]. It is therefore plausible to pose a question whether a given intensity time series is predictable, hence safe from eavesdropping before an eavesdropper contemplates to model the data and endeavors to forecast its development. The Hurst exponent is a numerical estimation tool for the predictability of a time series. It is defined as the relative tendency of a time series to either regress to a longer term mean value or cluster in a direction. The reason the Hurst exponent H is an estimate and not a definitive measure is because the algorithm operates under the assumption that the time series is a fractal, which is partly true for most chaotic time series. This is, however, of minimal importance and what really renders H such a valuable asset in such a qualitative analysis is that it provides a means of classifying time series in terms of predictability.

The values of the Hurst exponent range between 0 and 1. A Hurst exponent with value close to 0.5 indicates a random walk (a Brownian time series). In a random walk there is no correlation between any element and a future element and there is a 50% probability that future return values will go either up or down. Hence, series of this type are hard to predict and preferable for encryption techniques. A Hurst exponent value H between 0 and 0.5 exists for time series with "antipersistent behavior." The latter means that an increase will tend to be followed by a decrease (or inversely). This behavior is sometimes called "mean reversion" which means that future values will have a tendency to return to a longer term mean value. A Hurst exponent between 0.5 and 1 indicates "persistent behavior," meaning that the time series is trending. If for a time series X there is an increase from X_{t-1}

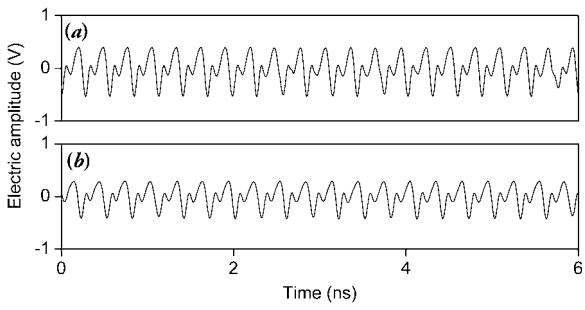

FIG. 3. (a) Zoomed periodic time-trace from Fig. 2(b) and (b) from Fig. 2(g), showing the beginning and the ending of the period-doubling sequences for the cyclic scenario.

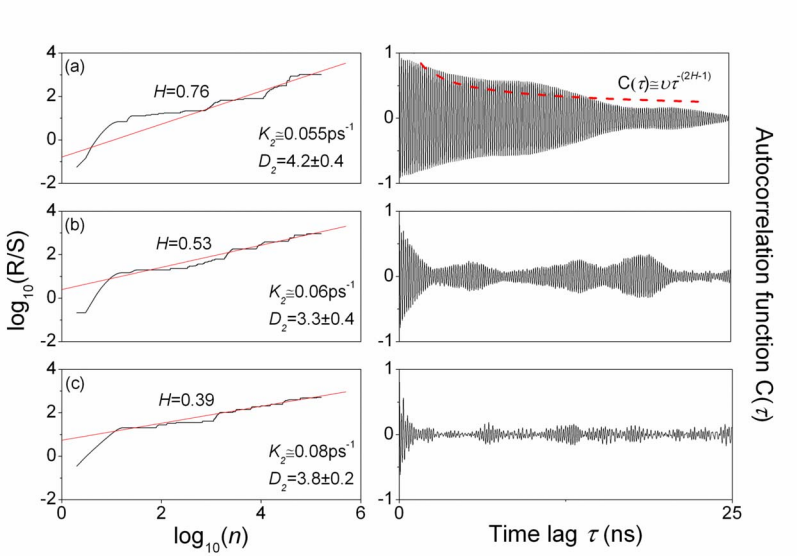

FIG. 4. (Color online) Left: Estimation of the Hurst exponent H following the R/S analysis. The depicted values of H are derived from the least squared fitted slopes. Right: Corresponding autocorrelation function for (a) $I_{\mathrm{PHs}}=2.6$ mA, (b) $I_{\mathrm{PHs}}=7.4$ mA, and (c) $I_{\mathrm{PHs}}=0.2$ mA. The multivariable fitting for the autocorrelation function "tails" in (a) results in $\upsilon=1.04$ and $H=0.73$.

to X_t there will probably be an increase from X_t to X_{t+1}. The same is factual for decreases, where a decrease will tend to follow a decrease and the larger the H value is, the stronger the trend. Series of this type are easier to predict than series falling in the other two categories and hence should abstain from encryption applications. It is professed that the Hurst exponent H ought not to be bewilderedly connected with the Kolmogorov entropy in a time-series analysis, albeit both quantifiers deal with predictability issues despite their discernible disparity. One is a time-domain property whereas the other is a topological property. Apropos of the above discussion regarding persistence and predictability, it is expected that series which fall in the range $0.5<H<1$ will typically result in smaller values of entropy, also demonstrated in Ref. [15] and shown next.

The *ab initio* calculation of the H exponent starts with applying the rescaled range (or R/S) analysis [8]. Each time series has a duration of 1 μs and consists of 1.6×10^5 points, therefore precluding significant statistical errors and erroneous estimates. One has to calculate the maximum excursion R from the starting point and divide it with the series' standard deviation. The H exponent is then equal to the slope of least-squares fitting of the maximum excursion and the number of recorded points n in a log-log diagram. All logarithm expressions herein are in base 10. In Fig. 4 we present three cases with $H>0.5$ [Fig. 4(a)], $H\approx0.5$ [Fig. 4(b)], and $H<0.5$ [Fig. 4(c)] together with their corresponding autocorrelation functions. It is interesting to observe that for long-term memory processes [$H>0.5$, Fig. 4(a)] the "tails" of the autocorrelation function $C(\tau)$ experience (roughly due to noise) a power scaling law $C(\tau)\approx\upsilon\tau^{-\alpha}$ where υ is a constant and $\alpha=2H-1$ [8], whereas for the two other cases it exhibits an erose trend, especially for $H<0.5$. The multivariable fitting resulted $\upsilon=1.04$ and $\alpha=0.46$, hence $H=0.73$, a value close to $H=0.76$ derived from the R/S analysis. The statistical standard error (SE) calculated for every case of H was close (but never larger) to $|\mathrm{SE}|<0.03$. The Kolmogorov entropy K_2 was additionally calculated together with the correlation dimension D_2 (as done in Ref. [7]) for each case resulting in $(H,K_2,D_2)=(0.76,0.055\ \mathrm{ps}^{-1},4.2\pm0.4)$ for Fig. 4(a), $(0.53,\ 0.06\ \mathrm{ps}^{-1},\ 3.3\pm0.4)$ for Fig. 4(b), and $(0.39,\ 0.08\ \mathrm{ps}^{-1},\ 3.8\pm0.2)$ for Fig. 4(c). The chaoticity K_2 appears to follow the H exponent in contrast to the complexity D_2 as also shown in Ref. [15]. Therefore, since H is much easier to calculate than K_2 it is anticipated to prove beneficial to experimentalists for qualitatively identifying the most chaotic and unpredictable regions. Of course, this is not always the case and some examples were found where H was not following K_2 consistently. Since the latter is greatly more difficult to calculate than H, it is concluded herein that H must be considered as an additional independent chaos quantifier and furthermore as a significant indicative measure for tracking maximized entropy. Moreover, its relation with the attractor dimension did not show any indication of correlation and this is something to be expected. It should be noted that the values of K_2 are greater than the ones calculated for the PIC in Ref. [7]. Most probably this has to do with the different DFB laser itself since it is known that different material parameters are able to easily result in different values for the chaoticity of a system. For example, especially for the linewidth enhancement factor that is known to dominate the chaoticity of an optically driven laser system [16], it is known that it increases as the wavelength rises and this increase is basically dependent on the carrier density due to the Coulomb enhancement effect. This is the case herein since the wavelength of the DFB laser is vaguely longer than the one studied in Ref. [7] expecting therefore different material parameters and hence different values for the entropy.

In Fig. 5 we present the effect of the feedback phase on the statistical properties of the attractor (kurtosis and skewness) and the calculation of the H exponent. The range of 0–10 mA for the current of the phase section could not be adequately calculated (in rads) since the repeat of the observed dynamics could not be noticed clearly, albeit it was deduced from specta observations to correspond approximately to a 2π phase change. The kurtosis K is the degree of peakedness of a distribution whereas the skewness S is a measure of the degree of lopsidedness of the latter in a time series.

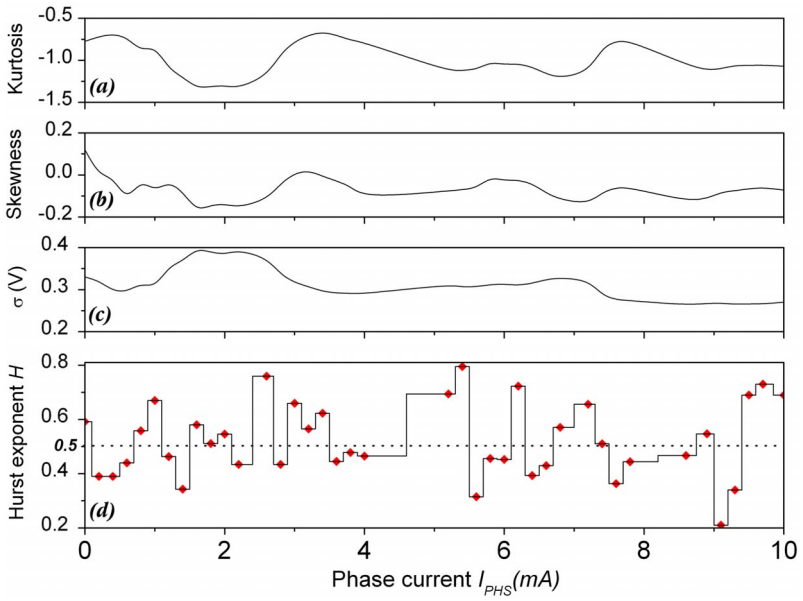

FIG. 5. (Color online) (a) Kurtosis, (b) skewness, (c) standard deviation, and (d) Hurst exponent H as the phase current I_{PHs} varies covering the range $0.2<H<0.8$. The calculated values are only for the diamonds depicted for the H exponent regarding only chaotic cases.

The standard deviation is also depicted since it is used in the H calculation. The skewness seems to remain relatively unaltered as the phase varies in contrast to the kurtosis exhibiting slightly more sudden local extrema. On the other hand, the H exponent is established to vary erratically above and below the value of 0.5. No specific correlation is expected for the H exponent with the two statistical quantifiers of kurtosis and skewness, but it is important for encryption applications to be able to tune the unpredictability quantifier (Hurst exponent) without simultaneously exhibiting notable variations in the chaotic carrier's statistical properties. Keeping the phase stable (for example, with variations $\Delta I_{\mathrm{PHS}}<0.1$ mA assuring a temperature-independent system) it is clear that one may choose safely the region to operate the PIC. For example, an optimal region is $7.5\ \mathrm{mA}<I_{\mathrm{PHS}}<9.2$ mA, where the H exponent is always $H\leqslant 0.5$. Additionally, the connected lines do not imply a fitting between the calculated values (with the diamonds) in the figure. The H exponent was calculated only for selected chaotic cases. Many regions of $H\leqslant 0.5$ exist, defined in the discussion above as most suitable for complexity issues. It is expected that as $I_{\mathrm{G/As}}$ increases, H will saturate to a value greater than 0.5 indicating thus persistent behavior as demonstrated in Ref. [10], but our results indicate that H can be retained close to 0.5 or even less if the phase is tuned appropriately. Lasers with long external cavities (as examined in Ref. [10]) generate more complex dynamics (high Lyapunov dimensions) and therefore considered apposite for chaotic communications. On the other hand, however, lasers with much shorter cavities—as in our case—are attested to be fully controllable and robust in operational regions that lead to less predictable chaotic carriers with $H\leqslant 0.5$, with simultaneously exhibiting high values of entropy, since the latter is known to saturate to a value independently of the cavity length for time-delayed systems [4]. It should be stated that the chaotic series were not filtered as in Ref. [7] since the predictability of the actual chaotic carriers is of interest. Nevertheless, it is expected that nonlinear filtering with state-space averaging would result in biased results for the H exponent in contrast to K_2 as demonstrated in Ref. [7] for noise-contaminated chaotic carriers. Depending on the signal-to-noise ratio (SNR), the exponent would be dominated by one or the other process (noise or chaos). Furthermore, filtering would typically change the exponent, and nonlinear filtering could accomplish almost anything. One should note that the H exponent is defined only for cases in which the probability distribution function follows a power law. That is usually the case with real-world noise and often the case for chaos, but certainly not always. Hence not any filtering attempt took place for these calculations.

In this paper we investigated some special dynamical characteristics of a photonic integrated circuit with respect to the field's feedback phase. A cyclic scenario was initially demonstrated. The variation of the phase furthermore resulted in minimal alterations in the statistical properties of the chaotic attractors and moreover revealed a variety of chaotic regions covering the range $0.2<H<0.8$. The Hurst exponent H is associated with the classification of a time series in terms of predictability, and therefore introduced as an additional important dynamical quantifier of a chaotic series in addition to the entropy and the dimension, whereas a qualitative connection with entropy was attempted. It was demonstrated that for the photonic integrated circuit described herein and first examined in Ref. [7], the dynamics are now pictured and may be tuned in the most desirable operating regions in terms of complexity (dimension), chaoticity (entropy), and predictability (Hurst exponent). The use of Hurst exponents in quantifying chaos and complexity in other experiments and in other fields is hence anticipated, together with the comparison of their connection with the metric entropy.

ACKNOWLEDGMENTS

This work was supported under EC Project No. PICASSO IST-2006-34551. The authors are indebted to the anonymous reviewers for their constructive comments towards the significant improvement of the paper.

[1] A. Argyris, D. Syvridis, L. Larger, V. Annovazzi-Lodi, P. Colet, I. Fischer, J. Garcia-Ojalvo, C. Mirasso, L. Pesquera, and K. A. Shore, Nature (London) **437**, 343 (2005).
[2] R. Roy, Nature (London) **438**, 298 (2005).
[3] H.-F. Chen and J.-M. Liu, Phys. Rev. E **71**, 046216 (2005).
[4] R. Vicente, J. Dauden, P. Colet, and R. Toral, IEEE J. Quantum Electron. **41**, 541 (2005).
[5] L. Larger, M. W. Lee, J.-P. Goedgebuer, and W. Elflein, J. Opt. Soc. Am. B **18**, 1063 (2001).
[6] M. Yousefi, Y. Barbarin, S. Beri, E. A. J. M. Bente, M. K. Smit, R. Nötzel, and D. Lenstra, Phys. Rev. Lett. **98**, 044101 (2007).
[7] A. Argyris, M. Hamacher, K. E. Chlouverakis, A. Bogris, and D. Syvridis, Phys. Rev. Lett. **100**, 194101 (2008).
[8] C. Sprott, *Chaos and Time Series Analysis* (Oxford University Press, Oxford, UK, 2003).
[9] H. E. Hurst, R. P. Black, and Y. M. Simaika, *Long-Term Storage: An Experimental Study* (Constable, London, 1965).
[10] Wing-Shun Lam, W. Ray, P. N. Guzdar, and R. Roy, Phys. Rev. Lett. **94**, 010602 (2005).
[11] T. C. Newell, V. Kovanis, and A. Gavrielides, Phys. Rev. Lett. **77**, 1747 (1996).
[12] K. E. Chlouverakis and M. J. Adams, IEEE J. Sel. Top. Quantum Electron. **12**, 398 (2006).
[13] M. Peil, I. Fischer, and W. Elsäszer, Phys. Rev. A **73**, 023805 (2006).
[14] A. Venkatesan and M. Lakshmanan, Phys. Rev. E **55**, 5134 (1997).
[15] A. Carbone and H. E. Stanley, Physica A **384**, 21 (2007).
[16] K. E. Chlouverakis, Int. J. Bifurcation Chaos Appl. Sci. Eng. **15**, 3011 (2005).